Towards Realistic Walk Path Simulation of Single Subjects

Presenting a Probabilistic Motion Planning Algorithm

Philipp Agethen
Daimler AG
Ulm, Germany

Felix Gaisbauer
Daimler AG
Ulm, Germany

Martin Manns
University of Siegen
Siegen, Germany

Max Link
Daimler AG
Ulm, Germany

Enrico Rukzio
Ulm University
Ulm, Germany

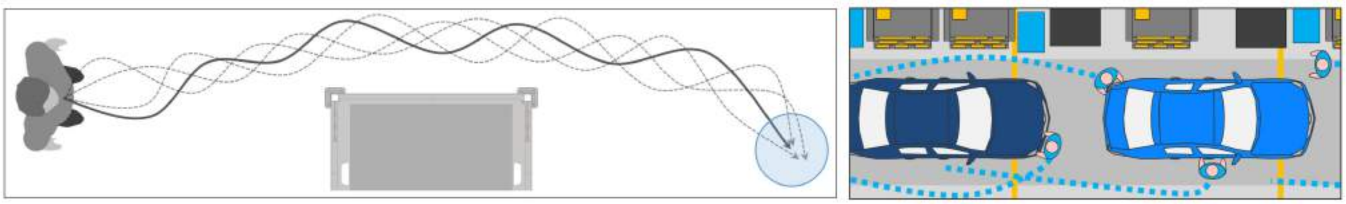

Figure 1: Overview of the proposed approach. Left side: statistically distributed locomotion trajectories. Right side: example of automotive walk path planning.

ABSTRACT

Within the manufacturing industry, digital modelling activities and the simulation of human motion in particular, have emerged during the last decades. For the use-case of walk path planning, however, recent path planning approaches on the one hand reveal drawbacks in terms of realism and naturalness of motion. On the other hand, the generation of variant-rich travel routes by means of modeling the statistical nature of human motion has not been explored yet. In order to contribute to a better prediction quality of planning models, this paper therefore presents an approach for realistically simulating walk paths of single subjects. In order to take into consideration the variability of human locomotion, a statistical model describing human motion in a two-dimensional bird's eye view is presented. This model is generated from a comprehensive database (20 000 steps) of captured human motion and covers a wide range of gait variants. In order to obtain short and collision-free trajectories, this approach is combined with a path planning algorithm. The utilized hybrid A* path planner can be regarded as an orchestration-instance, stitching together succeeding left and right steps, which were drawn from the statistical motion model. Although being initially designed for industrial purposes, this method can be applied to a wide range of use-cases beyond automotive walk path planning. To underline the evident benefits of the proposed approach, the novel motion planner's technical performance is demonstrated in an evaluation.

CCS CONCEPTS

• **Computing methodologies → Animation**; *Model development and analysis*; *Motion capture*;

KEYWORDS

Motion planning, probabilistic motion model, walk path planning, automotive production, spaghetti chart

ACM Reference Format:

Philipp Agethen, Felix Gaisbauer, Martin Manns, Max Link, and Enrico Rukzio. 2018. Towards Realistic Walk Path Simulation of Single Subjects: Presenting a Probabilistic Motion Planning Algorithm. In *MIG '18: Motion, Interaction and Games (MIG '18), November 8–10, 2018, Limassol, Cyprus.* ACM, New York, NY, USA, 10 pages. https://doi.org/10.1145/3274247.3274504

1 INTRODUCTION

The automotive industry is a highly competitive market. Manufacturers are currently facing the challenge of having to cope with a demand for product diversification, which leads to extensive product portfolios [Martín et al. 2013]. At the same time, this paradigm shift entails rising complexity for production since the total number of assembly tasks is growing. As a consequence of this ongoing process, digital simulation software have become indispensable in production planning, since traditional pen and paper methods are increasingly impracticable. Even though constituting a first step in the right direction, the outcome of industrial simulation software can significantly deviate from the situation on the shop-floor. Especially when planning the routes of assembly operators, simplifying assumptions of common path planning approaches are leading to a gap between plan and reality - as shown by [Agethen et al. 2016].

MIG '18, November 8–10, 2018, Limassol, Cyprus

ACM ISBN 978-1-4503-6015-9/18/11.
https://doi.org/10.1145/3274247.3274504

Most notably, these tools predominantly utilize algorithms (e.g., [Hart et al. 1968; Reynolds 1999]) neglecting gait and the statistical nature or human motion. In particular, a sequence of coarse-grained walk paths is simulated, which represents the average route of an assembly operator. Based on this trajectory, next, the expected mean distance and travel time is estimated. These information are in turn used for optimizing workplaces within manual assembly lines. However, this procedure does not consider the fact, that the spatio-temporal properties of each walk path varies statistically. For instance, each actual execution of a locomotion task is unique and slightly differs from the other counterparts. As a consequence, the sum of all walk paths being performed in the context of one nominal route (e.g., "walk from rack to car") does not show a deterministic behavior - but forms a statistically distributed motion corridor. Figure 1 depicts this phenomenon. Please note, that these circumstances intensify in the face of low cycle times for automotive production (approx. 100 s) and the high numbers of repetitions that come along with it.

Therefore, more precise and accurate methods for realistically modeling assembly workers' behavior have to be employed. To overcome these drawbacks, this paper presents a novel motion planning algorithm which is tailored to effectively generate statistically distributed root-joint trajectories. Even though being initially designed for the aforementioned use-case, the introduced methodology can be applied to a wide range of domains focusing on the simulation of single subjects.

In particular, the three main technical contributions of this paper are:

(1) A probabilistic motion model predicting the transition between succeeding left and right steps.
(2) The integration of this transition model into a hybrid A* path planning algorithm.
(3) The actual implementation of the novel motion planning algorithm.

The remainder of the paper is structured as follows: First, the state-of-the-art in the context of simulation of human locomotion is reviewed. Second, an approach is introduced to predict statistically distributed motion variations. In order to implement this principle for industrial purposes, a large number of human walking trajectories is captured using an OptiTrack motion capture system. Subsequently, a probabilistic motion model is presented, being derived from this database. Having introduced the novel approach, its applicability and technical performance is assessed in an evaluation. The paper concludes with an assessment and outlook on further optimizations.

2 RELATED WORK

The approach presented builds upon the following main research areas.

2.1 Motion Planning

In general, two-dimensional motion planning is utilized to generate a collision-free trajectory between the initial position of a virtual character and a target, while fulfilling certain constraints. In contrast to the domain of character animation, the whole locomotor system of the human body is reduced to its root-joint. Approaches in this domain can mainly be divided into local and global planners. Algorithms, which can be assigned to the latter category take into account knowledge about the entire scene, hence generating collision-free solutions on a global scale. In contrast, the former only guarantees local optimality, while minor computational costs are induced. Literature presents a wide range of approaches for local and global motion planning: amongst others, techniques such as cell decomposition [Hart et al. 1968], probabilistic roadmaps [Kavraki et al. 1996], potential fields [Gasparetto et al. 2015] as well as rapidly exploring random trees [LaValle 1998], genetic algorithms [Hu et al. 2004] or neural networks [Glasius et al. 1995] are used. Other works introduce steering behavior approaches [Reynolds 1999], physical models [Helbing et al. 2000] and velocity obstacle methods [Van Den Berg et al. 2011] or use vision-based approaches [Ondřej et al. 2010] to simulate human motion.

Even though literature presents algorithms (e.g., [Kavraki et al. 1996; LaValle 1998]), which are either based on statistical models or which utilize sampling-based approaches, none of those works address the vagueness of human locomotion. In contrast, probabilistic principles are predominantly chosen due to the high complexity of the search problem (e.g., robotics). Moreover, others investigate the stochasticity of human motion, however, solely in the context of crowds. For instance, Wang et al. [Wang et al. 2016, 2017] utilize Bayesian models to evaluate path patterns in crowds. Based on similar techniques, Yi et al. [Yi et al. 2015] on the one hand calculate statistically distributed travel times of multiple pedestrians. On the other hand, Musse et al. [Musse et al. 2012] develop an approach to compare crowds using velocity distributions. Although starting to consider the vagueness of human motion, current approaches are still limited to the use-case of two-dimensional crowd simulation. For modelling walk paths of single subjects, such probabilistic techniques are not in scope of literature so far. Furthermore, none of the aforementioned approaches explicitly addresses human gait and the probabilistic generation of realistic walk paths.

2.2 Data-driven Character Animation

In the field of character animation, several data-driven approaches exist, which amongst others utilize blending techniques [Bruderlin and Williams 1995], motion graphs [Kovar et al. 2002a], deep learning [Holden et al. 2017] or motion matching [Clavet 2016]. Even though achieving outstanding results in terms of naturalness, this paragraph only considers approaches being able to reproduce the vagueness of human motion.

In this context, literature presents various elaborate approaches, which model the fine-grained motion of each limb. By means of applying statistical motion models, it is furthermore possible to enabling the simulation of an infinite number of variants based on a restricted number of training data. In particular, literature presents a wide range of approaches utilizing different statistical models. This includes hidden Markov models [Bowden 2000; Tanco and Hilton 2000], linear time-invariant models [Hsu et al. 2005] and Gaussian Process Dynamical Models [wan [n. d.]]. More recently, Min and Chai [Min and Chai 2012] present an approach for probabilistically modeling of full-body human motion based on a motion capture database. Manns et al. [Manns et al. 2018] adapt this approach to the use-case of assembly planning. This representative overview of approaches underlines the high potential of probabilistic motion models for various use-cases. Instead of simulating one plausible motion, these algorithms allow to cover the full spectrum of human motion and the inherited vagueness.

Even though showing many evident benefits, the high dimensional models and complex processing pipelines show considerable requirements - both in quality and quantity - with regard to the utilized motion capture data sets [Manns et al. 2016a,b]. In contrast, the problem of generating realistic root-trajectories comprises a significantly reduced number of dimensions. In fact, most of the information being contained in such models is not needed for the use-case of walk path simulation. For instance, the approach presented by Manns et al. [Manns et al. 2018] utilize motion capture data with ≈ 80 dimensions per frame, whereas the introduced model is based upon 2D root-trajectories.

2.3 Footstep Planning

A third relevant domain of previous work is footstep planning. Being located between character animation and path planning, this cluster aims at planning an optimal sequence of foot contact points. Subsequently, the thus obtained footsteps can either be used to animate a virtual character or to navigate a robot through an unknown environment.

In the context of computer graphics, Choi et al [Choi et al. 2003] present an approach to determine footprints using probabilistic roadmaps. Moreover, multiple works (e.g., [Egges and van Basten 2010; van Basten et al. 2011; van de Panne 1997]) generate biped locomotion using sequences of contact points. More recently, Agrawal and van de Panne [Agrawal and van de Panne 2016] demonstrate how to on the one hand plan footsteps while taking task-specific context information into account. On the other hand, they subsequently generate realistic fully-articulated motion using an inverse kinematics. Furthermore, a large body of previous work investigate biped motion planning algorithms in the context of robotics. In particular, multiple works (e.g, [Chestnutt et al. 2003, 2006; Kuffner et al. 2002]) present approaches combining finite gait transition sets with various path planning algorithms. A detailed overview can be found in [Perrin 2018].

In general, approaches as presented in [Agrawal and van de Panne 2016; Choi et al. 2003] are ideally suited to plan footsteps between a start and a target configuration. However, the root motion is only approximated based on the optimized sequence of floor-contact points in a subsequent step. Consequently, the problem of directly generating realistic root-trajectories in two dimensions is still unsolved. Moreover, none of the aforementioned approaches considers the statistical nature of human motion. Same applies for the field of robotics, which utilizes a finite set of possible steps to generate collision-free motions. Nevertheless, the idea of combining a transition model with a path planning algorithm forms the basis for this paper. In particular, this paper builds upon the inspiring work of Chestnutt et al [Chestnutt et al. 2006].

3 CONCEPT

In industrial production, walk paths are planned in a bird's eye view, while the operator's traveled distance is taken into account to assess the efficiency of the assembly workplace. In this context, the fully-articulated human body composing several joints and dimensions is reduced to its root. For the sake of feasible modelling and planning effort, current process plans do not consider human gait and its resulting sinusoidal shaped root-trajectory. Furthermore, the fact that the same motion will be performed differently by a group of subjects (i.e., inter-variance) is also neglected. Same applies for the intra-variance. In order to take into account the aforementioned aspects, this paper presents an approach combining a hybrid A* path planner [Petereit et al. 2012] with a statistical motion model, which is inspired by Min and Chai [Min and Chai 2012]. Additionally, the approach incorporates a motion planner, the hybrid A* star algorithm [Petereit et al. 2012], to obtain short and collision-free trajectories between a start and a goal configuration. Using this novel algorithm, realistic root-joint trajectories of single subjects can be simulated. As the proposed approach considers both, the statistical nature of human motion and effects being induced by gait, it is possible to effectively generate a rich repertoire of realistic walking trajectories.

3.1 Overview

In general, the proposed approach can be sub-divided into four fundamental steps. In a first step, movements of actual persons are recorded using a motion capture system. The result of this are whole takes of continuous and fully-articulated motions. Human locomotion generally consists of sequences of succeeding left and right steps. Therefore, the data is afterwards fragmented into those atomic motion segments. These segments are hereinafter also referred to as motion primitives. Having obtained an adequate database, it can be used for synthesis of new motions by means of stitching together succeeding left and right steps [Kovar et al. 2002b]. To exclusively concatenate adequate motion segments from the database, a hybrid A* path planning algorithm is utilized to find suitable solutions to given motion planning problems - without violating any collision-constraints. To take into account the variation in human locomotion, each utilized motion primitive is drawn from a statistical motion model [Manns et al. 2018; Min and Chai 2012]. In particular, a transition model (i.e., Gaussian processes) for succeeding motion primitives is trained, which allows sampling of novel physically feasible and reasonable motions. The following gives a detailed description of the algorithm and the necessary steps.

3.2 Motion Capture

In order to obtain a database for the subsequent steps, first, motion capture data have to be acquired. In the context of this paper, motions stemming from 12 participants were recorded. For this purpose, an OptiTrack motion capture system (120 Hz) was utilized. Each participant was equipped with 37 retroreflective markers, in order to obtain sufficient detail for movements of crucial body parts (hip region as well as the feet). Subsequently, the root was projected onto the floor plane in order to be compatible with two-dimensional motion synthesis. In total, an area of $3.3\ m \times 3.2\ m$ could been tracked using the described setup.

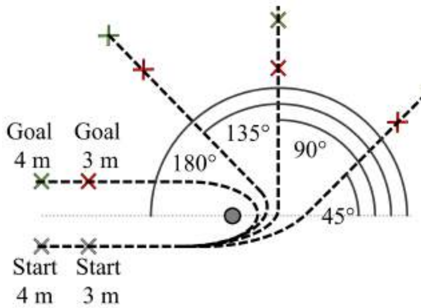

Figure 2: Setup of experiment: (1) Participants walked freely in the rectangular tracking space. (2) Participants walked around a pole for varying angles and distances. (3) The identical group walked along a straight line in a range between 3.0 m and 4.0 m (not shown).

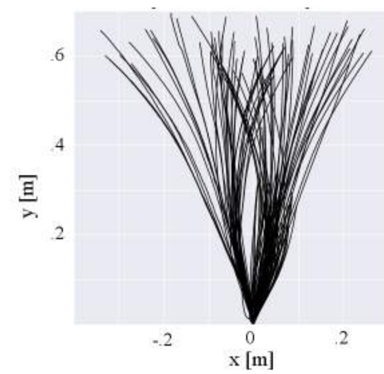

Figure 3: Motion segmentation results: Single motion segments of one experiment, performed by a specific subject.

To cover a large motion variety and to consider, both intra- and inter-subject variance, 12 healthy persons participated in an experiment. The group comprised 5 female and 7 male and showed following statistics: age: $\mu = 24.4$, $\sigma = 1.8$ and height: $\mu = 1.75\ m$, $\sigma = .04\ m$. In order to not obstruct the walking style, participants wore their own clothing and shoes. None of the participants reported vision or balance disorders.

Moreover, the experiment consisted of three main scenarios:

(1) Walking around freely in the rectangular tracking space while varying speed and curvature for 4 min. This includes side steps as well as turn steps.
(2) Walking straight lines with path lengths of 3 m and 4 m, respectively, for a duration of 2 min each.
(3) Walking straight towards a pole, passing it, turning by a certain angle, then walking straight again for angles of 45°, 90°, 135°, and 180°, respectively, each for path lengths of 3 m and 4 m (see Figure 2). The duration of each experiment was 2 min.

Overall, a total amount of 5 h of walking could be captured, which corresponds to $\approx 20\ km$ of walking distance.

3.3 Motion Segmentation

In order to obtain single motion segments that can be used for modeling walk paths, the recorded motion has to be decomposed. To determine segments where movement characteristics are uniform in some sense (see [Buchin et al. 2011]) the human gait cycle is initially analyzed:

In general, a walking motion consists of a succession of alternating left and right steps. A step can be divided into two phases, the stance phase and the swing phase, respective to each foot. The stance phase starts when the heel of the right/left foot touches the floor, initiating a phase of double support - at this time, both feet contribute to carrying the weight of the body. Then, when the right/left foot is fully loaded, the remaining foot is left off the ground and swung forward. During the left/right foot's swing phase, the opposite foot is single supporter of the body's load. Then, when the left/right heel touches the ground again, the course of action described above is repeated with both feet interchanged.

Hence, the walking motion is divided into segments by means of detecting changes in foot contact with the ground. The frames where these changes occur are denoted as key frames. In order to obtain those frames, the speed and z-value (elevation) of both feet is monitored. Both values approach zero when a foot is fully loaded. When the foot is lifted from the ground, speed and the z-value of the toes take on positive values. Thus, key frames can be found by identifying changes in these features using an adaptive threshold (scipy [Jones et al. 2001], function *gaussian_filter1d*, $\sigma = 180$, offset = 5^{th} percentile).

When key frames have been extracted from the motion capture data, the result is a set of segmented root-trajectories representing left and right steps, respectively. For later use, the root-trajectories are aligned in a way that they all start in the origin of the horizontal plane. Furthermore, the trajectories are rotated towards the up-axis so that the hip's starting orientation points into the same direction.

In total, the database of $\approx 20km$ (see section 3.2) of walking is thus automatically segmented into approximately 20 000 steps. Figure 3 shows an example of segmented and aligned trajectories stemming from one specific subject (both left and right steps).

3.4 Motion Synthesis and Path Planning

After the motion has been divided into single segments, the resulting set of left and right steps can be used to generate realistic paths from a start to an end point. Following Kovar et al. [Kovar et al. 2002b], a complex motion can be generated by means of connecting multiple motion primitives (or elementary motions). Transferred to human locomotion, a walk trajectory can be composed from a series of gait cycles and succeeding steps. However, the arbitrary combination of different primitives will lead to unnatural results. In particular, the end of each primitive has to match the beginning of the subsequent counterpart in terms of continuity of motion. Otherwise, the discontinuity will become visible in a jerk movement, which results in an unnatural seeming trajectory. Moreover, pairs of primitives must be physically feasible and reasonable. In particular, even if two motion primitives fit together well in regard to continuity of positions, some concatenations will lead to inconsistencies. This refers to mainly two properties of motion, namely speed and direction of heading. For instance, a sharp turn would seem unnatural for high walking speed and moreover, would physically not be feasible due to mass inertia of the human body.

In order to meet these criteria, a multidimensional function approximation is used to model the relationship between motion primitives and their corresponding predecessors. In this paper, this is archived by means of fitting a statistical model to the captured ≈ 20 000 transitions between consecutive steps (training data). Following Min and Chai [Min and Chai 2012], Gaussian Processes (GP) are used for this purpose as they are able to efficiently model non-linear properties of transition functions, while the learning process only involves very few tuning parameters. To obtain continuous and physically feasible transitions as input data, the GP-model is trained using pairs of motion primitives, which have actually be captured in succession (during section 3.2). Naturally and by definition, those pairs of predecessors and successors are reasonable, feasible and continuous, since they have in fact been performed by real human subjects. Having trained the GP-model, it is possible to obtain a novel continuous, physically feasible and reasonable motion primitive for given predecessors by means of drawing samples.

As the initial step within each trajectory has no predecessors, the trained transition model cannot be used to sample the first motion primitive. Consequently, a second generative model has to be constructed, which enables to independently generate motion primitives - similar to those depicted in Figure 3. Therefore, a kernel-density estimation (KDE) is used, which is a non-parametric statistical approach for modelling random variables. The underlying principle is that each observed data point creates its own local density function using a kernel function (in this case a Gaussian Kernel). The estimated density at an arbitrary data point can then be calculated as the mean density given by the kernel function. The Gaussian KDE-model allows for sampling data which is near to the original, but still showing variance.

The interplay between both statistical models is implemented as follows: First, the Gaussian KDE approach samples an initial motion primitive. Next, the GP-model uses this first step as input to predict a continuous and physically feasible successor. Having generated a second motion primitive, the last step is in turn used to simulate a third gait cycle. This procedure is repeated until the target point is reached. Figure 4 illustrates this proposed approach. It can be seen, that the walk path of a virtual human is generated by means of stitching together succeeding left p_L and right p_R steps.

Even though each generated atomic root trajectory will fit to its preceding counterpart, an arbitrary combination of p_i might not lead to the target destination - or violate collision constraints. Figure 4 depicts this problem. Some of the six sampled motion primitives $p_{R,1,\dots,6}$ will lead to detours (e.g., $p_{R,1}$, $p_{R,2}$ and $p_{R,5}$), or might result in unnecessary short stride lengths (see $p_{R,3}$). Therefore, both statistical models are integrated into a hybrid A* [Petereit et al. 2012] path planning algorithm. Similar to the A* approach [Hart et al. 1968], this adapted version divides the scene into cells and optimizes transitions between cells using a heuristic function. In contrast, the hybrid A* also allows continuous positions within cells, which enables the assessment of each motion primitive's end point. In general, the sampled p_i trajectories define all possible actions within each expand step. Metaphorically, each sample's suitability for a given search problem can be determined using the hybrid A* methodology. For Figure 4, this iterative process would accept $p_{R,4}$.

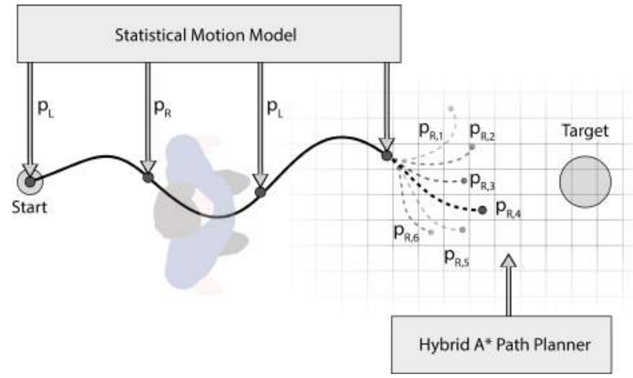

Figure 4: Concept of proposed algorithm: A statistical motion model samples multiple feasible motion primitives which are assessed using the Hybrid A* path planner.

Next, the GP-based sampling process will be repeated using $p_{R,4}$ as new predecessor.

4 IMPLEMENTATION

In this section, the algorithmic implementation of section 3.4 is explained. An overview in pseudocode is given in 1.

4.1 Preprocessing and Model Fitting

To train both, the KDE- and the GP-model, the segmented motion capture dataset is initially preprocessed. This step mainly ensures an efficient and robust fitting of the model to the training dataset. In particular, each trajectory is initially represented by a B-spline in order to counterbalance the effect of outliers and to further reduce the number of dimensions [Min and Chai 2012]. For this purpose, the path is subdivided into five equidistant spaces. The resulting landmarks are used to build the B-spline upon (function *BSpline* [Jones et al. 2001]). Next, a Principal Component Analysis (PCA) is performed in order to exclude unnecessary information. The idea of PCA is that, given a set of data in the high dimensional space, an affine lower dimensional subspace is to be found, that contains most of the variance of the original data. This kind of linear dimensionality reduction is done using Singular Value Decomposition. Therefore, the Python library *sklearn* (function *PCA*, *svd_solver = full*) is used [Pedregosa et al. 2011]. Thus the data is projected into a subspace, which contains at least 95% of the variance of the data. Subsequently, the single features of the data in subspace are standardized by setting the mean to $\mu = 0$ and scaling the data to unit variance ($\sigma = 1$) using the function *StandardScaler* [Pedregosa et al. 2011].

Afterwards, both generative models are trained. For the kernel-density estimation the function *gaussian_kde* of the Python library *scipy* [Jones et al. 2001] is used while the Gaussian Process Regressor is implemented by *sklearn* [Pedregosa et al. 2011]. For the GP-model, a prior needs to be specified. Its mean is assumed to be constant and zero; its covariance is specified by a Radial-basis function kernel, whose hyperparameters are optimized during fitting by maximizing the log-marginal-likelihood (LML). Afterwards the

Gaussian Process Regressor is able to find a feasible successor for a given predecessor as described above. For a specific set of motion primitives, the preprocessing steps have to be carried out only once; the PCA, scaler and parameters of the Gaussian Process Regressor are saved in order to reverse the steps when a successor primitive has been drawn.

4.2 Initialization and Exploration Loop

Having trained both models, motion synthesis is performed at 120 fps. For this purpose, first, the start configuration is transformed to a corresponding node n_s with zero cost ($g = 0$), no predecessor and information about its heuristic value as well as its cell position and index. The heuristic h used is defined to be the two-dimensional Euclidean distance (straight-line) from the respective position to the center of the goal area. Furthermore the open list O, which is implemented as min-heap, is being initialized by inserting the starting node n_s. Initially, the closed list is empty.

Next, the exploration loop is iteratively performed. As described above, the KDE is model is utilized to randomly sample 30 left and right starting steps. Once multiple feasible transitions have been sampled, the algorithm successively explores the node n_{best} with least estimated total cost f. This node is removed from O and its index is added to the closed list C. If the position of n_{best} lies within the goal area G (tolerance of .25 m), the algorithm terminates. In this case, the root-trajectory is determined by means of traversing the constructed search-tree from leaf (= n_{best}) to root (= n_s), while concatenating the transitions (i.e., motion primitives). Otherwise, the node is expanded and a list of feasible successors is appended to the path, if they do not end in a cell whose index is in the closed list. In all subsequent iterations, the Gaussian Process Regressor uses the most suitable root-trajectory to, in turn, generate 10 potential transitions between cells (see Figure 4).

To derive a trajectory from the set of features created by the KDE- or GP-Model, the first three preprocessing steps are reverted: First, the data is scaled back. Afterwards, the data is transformed back to its original space **S**, and lastly, the B-spline is evaluated. The result is a trajectory in a local coordinate system, starting in the origin and heading in the direction of the up-axis. In order to append a trajectory to its predecessor, it has to be converted from the local coordinate system to the global coordinate system. This is done by rotating the trajectory so that it fits the heading of its predecessor and translating the trajectory so that it starts where the preceding motion primitive has ended.

5 EVALUATION

In order to assess the technical performance of the proposed approach, a two-staged evaluation is performed.

5.1 Assessment of Technical Performance and Generated Trajectories

Figure 5 shows 15 trajectories in a bird's eye view being generated for an exemplary scene, comprising a starting configuration (top left corner), a goal region (bottom right corner) and a number of obstacles that have to be avoided by the novel path planner. For this scenario, a cell size of .08 m was used.

Algorithm 1 Path Planner

Input: Start and end configuration with constraints motion primitives ($\mathbf{x}_s, G, m, \boldsymbol{\nu}$)
Output: Collision free path from start configuration to end configuration

procedure PREPROCESSING($\boldsymbol{\nu}$)
    $\boldsymbol{\nu}_{spline} \leftarrow$ representation of all motion primitives in $\boldsymbol{\nu}$ as cubic B-splines
    $\boldsymbol{\nu}_{pca} \leftarrow \boldsymbol{\nu}_{spline}$ after PCA
    $\boldsymbol{\mu} \leftarrow$ standard scaled $\boldsymbol{\nu}_{pca}$
    create KDE for beginning steps
    create GP-model for transitions between different kinds of motion primitives
    return $\boldsymbol{\mu}$, KDE, GP

procedure FINDGOAL($\mathbf{x}_s, G, m, \mu, KDE, GP$)
    initializeAlgorithm($\mathbf{x}_s, m, KDE$)
    repeat
        pick n_{best} from O such that $f(n_{best}) \leq f(n), \forall n \in O$.
        remove n_{best} from O and add index $\tilde{\mathbf{x}}_n$ to C.
        if n_{best} in G **then** EXIT.
        Expand n_{best}: $\mathbf{x} \leftarrow$ findFeasibleSuccessors(n_{best}, GP)
        for all *successor* **in x do**
            append *succ* to n_{best} **if not** ($\tilde{\mathbf{x}}_{succ}$ in C **or** $m(\tilde{\mathbf{x}}_{succ}) == True$)
    until O is empty

procedure INITIALIZEALGORITHM($\mathbf{x}_s, m, KDE$)
    $n_s \leftarrow (\tilde{\mathbf{x}}_s, \mathbf{x}_s, 0, h(\mathbf{x}_s), -)$
    $O \leftarrow n_s$
    $C \leftarrow \emptyset$
    for i=1,2,...,#$starters$ **do**
        resample from KDE-model for beginning steps
        append resample to n_s **if not** ($\tilde{\mathbf{x}}_{succ}$ in C **or** $m(\tilde{\mathbf{x}}_{succ}) == True$)

procedure FINDFEASIBLESUCCESSORS(n_{best}, GP)
    draw samples from GP transition distribution for the trajectory of n_{best}
    for sample **in** samples **do**
        Reverse Scaling: Scale sample back
        Reverse PCA: Transform data back into its original space
        Transform spline representation into trajectories
    return trajectories

First of all, it can be seen, that on the one hand, smooth and short paths are obtained, connecting the start and the target region. On the other hand, none of the generated results violates any collision-constraints. Most importantly, each of the 15 trajectories is unique and differs from the remaining counterparts within a motion corridor. It can thus be confirmed that the proposed algorithm is able to reproduce the statistical nature of human locomotion by means of generating statistically distributed trajectories.

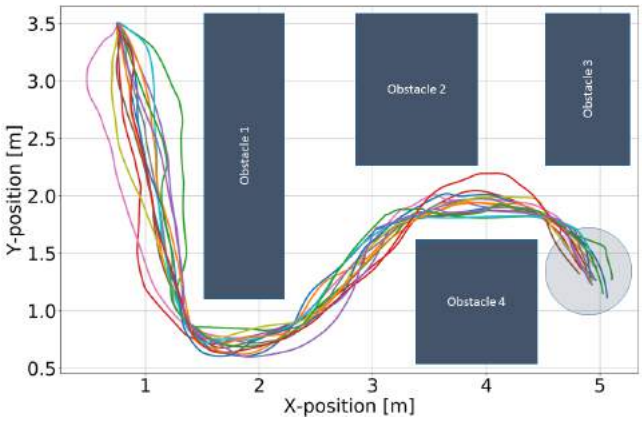

Figure 5: Macroscopic results of the proposed approach in a bird's eye view: 15 randomly sampled root-trajectories between a start and a target configuration.

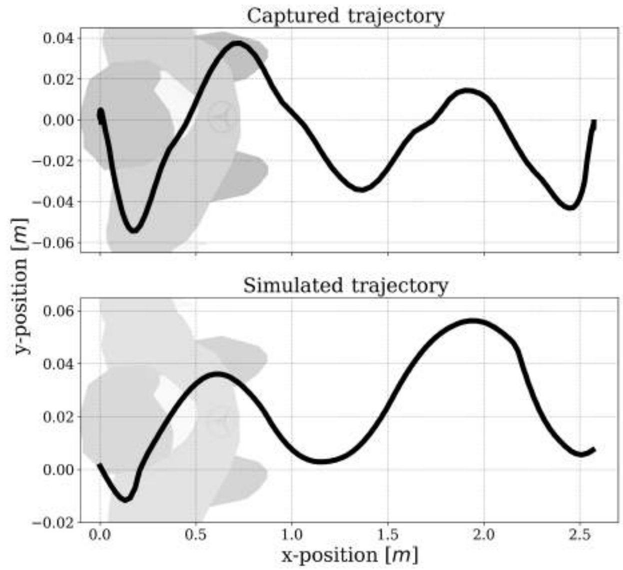

Figure 6: Microscopic results of the proposed approach in a bird's eye view: two detailed representation of a captured and a simulated trajectory which consider gait.

Furthermore, Figure 6 depicts two exemplary root-trajectories with a distance of 2.5 m. Note that the plots are not scaled uniformly, in order highlight the effects of gait on the walk path. The upper half represents a captured motion from the KIT Whole-Body Human Motion Database [Mandery et al. 2015], whereas the lower sub-plot depicts its simulated counterpart. Comparing the routes, it becomes apparent that the proposed planner explicitly considers the human gait-cycle, as both root-trajectories show a similar sinusoidal shape. This can be mainly traced back to the underlying sampling principle generating alternating left and right steps. Even though reproducing effects being related to gait, the artificial walk path shows a slightly different shape. A possible reason for this is the fact, that varying motion patterns can be observed for different subjects, which are unique for each human. Moreover, both motions can be decomposed into 5 primitives (= 5 steps), while the artificial trajectory comprise smooth and feasible transitions. Summarizing the aforementioned findings, it can be stated that besides addressing the vagueness in human locomotion, the novel motion planner also reproduces effects being related to gait.

Performed on an Intel i7-6820HQ with 2.70 GHz, the proposed probabilistic motion planning algorithm allows the generation of 8 m (see Figure 5) walk paths in approximately 5 s. Transferred to the use-case of industrial walk path planning, the simulation of a representative assembly workplace comprising five walk paths would take half a minute. This can be regarded to be reasonable. However, compared to a mean computation time of .5 s, for generating similar root-trajectories using a standard A*, it becomes apparent that a more efficient implementation of the GP-model could significantly increase the overall-performance. Please note that a slightly modified implementation (discrete cells) of the utilized Hybrid A* algorithm was used to benchmark the novel approach.

5.2 Compassion to State of Art and Captured Human Motions

Besides visually analyzing generated root-trajectories, the proposed algorithm is also compared to a state of art planner and a large database of captured human motion. In order to obtain an adequate set of walk paths, first, 10 participants were recruited. In particular, the group showed following characteristics: 9 male and 1 female being aged from 21 to 40 ($\mu = 27.80$, $\sigma = 6.08$) with a height ranging from 1.60 m to 1.98 m ($\mu = 1.79\ m$, $\sigma = .12\ m$). None of the participants reported vision or balance disorders.

Next, a representative assembly station is set up, which comprise one car and three racks (see Figure 7), each containing two screws. Based upon this apparatus, a list of assembly tasks is subsequently defined. In particular, first, each subject started at rack 2 and successively carried and fastened the two screws to the car at a self-selected speed. Next, the same procedure was repeated for rack 3 and 1. Finally, the operator had to carry a tool from rack 2 to 3. This set of assembly tasks was repeated 10 times by each participant.

During the experiment the participants' root-joints were monitored using an HTC Vive tracking system (update rate 60 Hz). In particular, a controller was placed on the front side in center of the participant's hip (i.e., umbilicus) with the help of an elastic belt. The root was subsequently derived for each participant as the extension of the controller's z-axis while taking into account half of the torso depth and the distance between controller and skin.

Having conducted the experiment, the 10 participants generated a database of 1984 point-to-point walk paths with an overall-length of 4.06 km. In a subsequent step, the captured scenario is simulated while taking into account the knowledge about number of captured trajectories and the position and dimension of all obstacles. Besides the presented algorithm, the evaluation also comprised two state of the art approaches in order to ensure comparability. In particular, an A* path planner is utilized to simulate the identical scene (similar implementation as the proposed algorithm). Again, a cell

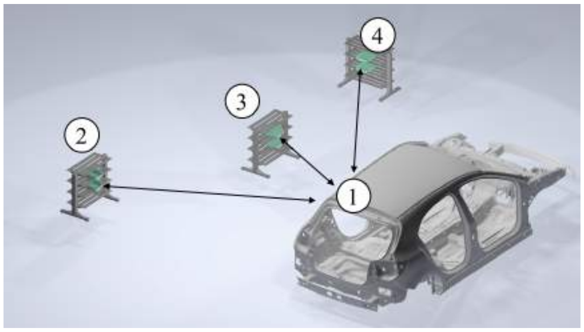

Figure 7: Setup of the representative workplace, which is utilized to benchmark the proposed algorithm.

size of .08 m was used. Moreover, the fully-articulated motion of a data-driven character animation approach being presented by Holden et al. [Holden et al. 2017] is also compared to proposed algorithm. In particular, the implementation of Sebastian Starke[1] was used, which followed the planned A* trajectories. Note that in all subsequent steps, only the root joint is utilized.

Figure 8 depicts the results of this evaluation in a bird's eyes view: The upper left side depicts the outcomes of the deterministic A* approach, whereas the upper right section represents the trajectories, being generated by [Holden et al. 2017]. The lower left side shows the trajectories being generated using the proposed algorithm, while the corresponding right side illustrates the captured baseline. Grey boxes illustrate the positions and dimensions of the utilized racks and the car (see Figure 7).

It becomes apparent, that the A* and the character animation approach (see upper half of Figure 8) do not generate statistically distributed motion corridors, even though each of the four subplots comprises the same number of walk paths. When being executed multiple times, rather, both algorithms simulate an identical set of walk paths for a given planning problem. The reason for this finding lies in the deterministic nature of both path planning algorithms, which does not allow to cover the vagueness and variant-richness of human locomotion (using identical input parameters). In contrast, the proposed probabilistic algorithm (see lower left section in Figure 8) reproduces the widespread motion corridor of the baseline. Interestingly those bundles of trajectories on average follow the routes, being generated by the A* algorithm. This is mainly due to the fact, that the novel planner inherits a derivative of the state of art approach (i.e., hybrid A*) in order to determine feasible successors. Consequently, it can be concluded, that the GP- and KDE-model metaphorically enrich the A* trajectory.

Furthermore, the walk paths being determined using the A* algorithm show sharp and unnatural turns while gait is not considered. Even though the trajectory might be post-smoothed [MAN 2015], the two remaining aspects (i.e., gait and vagueness) will still remain undressed. In contrast, the upper right side of Figure 8 reveals, that the character animation method [Holden et al. 2017] generates realistic and smooth walk paths, which show a sinusoidal form. Similar results can be observed for the novel approach - as shown in Figure 6.

[1]https://github.com/sebastianstarke/AI4Animation

To compare the baseline trajectories and the three artificial sets of walk paths, the Euclidean cloud-to-cloud distance is calculated for each pair : baseline ↔ A*, baseline ↔ [Holden et al. 2017] and baseline ↔ proposed approach. For this purpose the tool CloudComparer [CloudCompare 2018] is used. Low error values indicate that a tested set of trajectories geometrically overlaps and thus covers the same area. This in turn is mainly affected by, the shape of the routes and the geometrical variability (i.e., breadth of motion corridor). Consequently, the cloud-to-cloud distance on the one hand measures similarity in terms of geometric variance and variability of motion. On the the other hand, the shapes of the generated trajectories are further taken into account.

According to a performed Kolmogorov-Smirnov test (SPSS), all three pairs show non-normal error distributions (i.e., $p = .000$) and following descriptive statistics: baseline ↔ path planning: 50^{th} percentile .091 m and interquartile range (IQR) .113 m. Baseline ↔ character animation: 50^{th} percentile .065 m and IQR .098 m. Baseline ↔ proposed approach: 50^{th} percentile .002 m and IQR .002 m. Comparing the path planning with the character animation approach, a considerable median error reduction of 29 % can be observed. A performed Wilcoxon signed-rank points out statistically significant results (i.e. $p = .000$, $1 - \beta = 1.0$). This can mainly be attributed to the consideration of gait and the realisitic root trajectories. Comparing the error distributions of the proposed and the A* planner, the cloud-to-cloud distances point out a error reduction of 98 %. The Wilcoxon signed-rank test indicates statistical significance (i.e. $p = .000$, $1 - \beta = 1.0$). This underline the previous findings, that the proposed approach outperforms the state of art in terms of geometrical motion corridor coverage.

To further disaggregate this enhancement, each of the five different walk path (T1 to T5, see Figure 8) is analyzed separately with respect to its length. Table 1 summarizes the distribution for each of the five walk paths T1 to T5. Comparing the median of the baseline and the A*, it becomes apparent, that the path planner overestimates the distances - except for T5. This delta of up to 11 % mainly stems from the artificial trajectory's sharp turns, which increase the distance. The character animation approach considerably reduces this deviation, which can be attributed to the realistic root trajectory, considering gait. However, please note, that both algorithms solely determine a single walk paths, without generating variance (see IQR). Finally, the proposed approach predicts the median length with a similar deviation compared to [Holden et al. 2017]: 1 % to 4 %. However, it is noteworthy that T5 points out a considerable deviation. This is due to the fact, that the motion model is mainly trained using longer walking distances comprising larger stride lengths. As a consequence, a short path of ≈ 1 m is very likely to be simulated using a single step of .8 m - even though two short steps would be more suitable. Comparing the IQR, it becomes apparent that the proposed algorithms predicts between 60 % and 90 % of the captured variance. Given the two-dimensional motion model, which does not considers the influence of task-based locomotion (see [Agrawal and van de Panne 2016]), this result can be regarded as sufficient.

Transferring these finding to the initially mentioned use-case of automotive production planning, the A* path planner seems unsuitable due to the overestimation of distances. In contrast, the

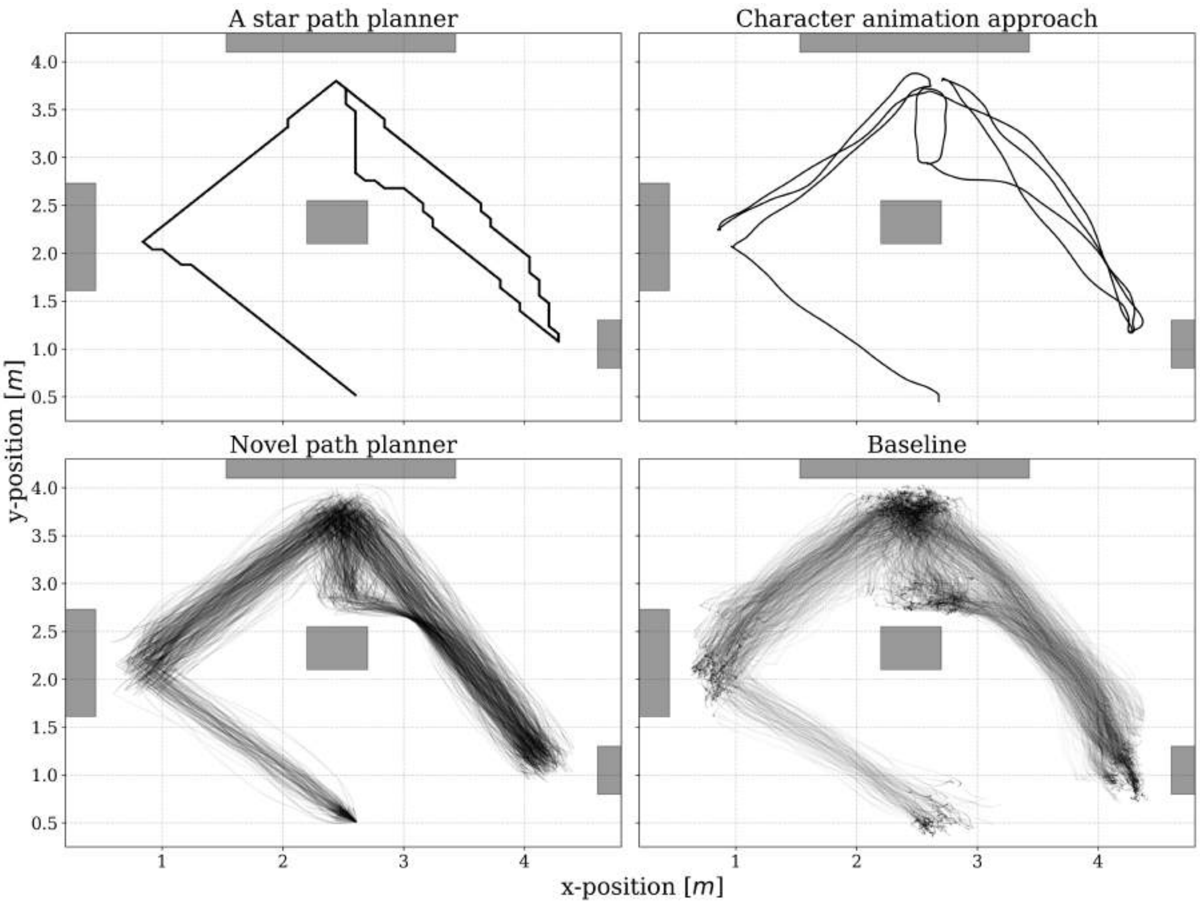

Figure 8: Overview of the results; top row: motion corridors being generated by the A* path planner and the character animation approach [Holden et al. 2017]; lower half: results of the proposed algorithms (left) and the captured baseline (right).

Table 1: Walk path length distribution for each of the five walk paths T1 to T5, being depicted in Figure 8: median and interquartile range in meters.

Distribution walk path length [m]								
	Baseline		A*		[Holden et al. 2017]		Proposed	
	50^{th}	IQR	50^{th}	IQR	50^{th}	IQR	50^{th}	IQR
T1	2.38	.21	2.42	-	2.41	-	2.41	.16
T2	2.25	.40	2.34	-	2.36	-	2.35	.24
T3	3.15	.38	3.48	-	3.28	-	3.11	.21
T4	2.44	.34	2.60	-	2.46	-	2.43	.21
T5	1.07	.21	.99	-	.97	-	.80	.23

character animation approach precisely reproduces the average walking behavior, however, neglects the vagueness of motion. This problem can be solved using the introduced approach, as it covers the predominant proportion of variance. Accounting for this variability can help to identify problems, which only occur as a consequence of accumulated statistical effects. Given the high numbers of repetitions in automotive production, even the observed variance of ≈ 14 % (ratio IQR and median walk path length) might lead to production disruption - since it is not considered in process plans. As a matter of fact, average process plans can over- or underestimate the actual performance of an assembly line, which potentially leads to overexertion of assembly operators. This underlines the potential of utilizing probabilistic motion planning algorithms for industrial applications.

6 CONCLUSION AND FURTHER WORK

This paper presents an approach that combines a hybrid A* path planner with a statistical motion model to effectively generate a rich repertoire of walking trajectories. The motion model is generated from a comprehensive database (20 000 steps) of captured and segmented human motion and covers a wide range of gait variants. The hybrid A* path planner can be regarded as an orchestration-instance, stitching together succeeding left and right steps, which were drawn from the statistical motion model. Moreover, the hybrid A* planner ensures a collision-free path between a start and an end point. Summarizing the findings of the two-staged evaluation, it can be concluded that on the one hand side, the data-driven motion model enables the generation of realistic sinusoidal shaped trajectories. On the other hand, the chosen Hybrid A* path planner ensures the combination of meaningful motion primitives, hence generating short and collision-free paths. Most importantly, the chosen probabilistic model is able to cover a wide range of motion variations, which significantly increase the prediction quality of two-dimensional motion planning of single subjects.

Future work will concentrate on extending and optimizing the presented algorithm. In this context, it is planned to enhance the exploration loop by means of introducing artificial potential fields. The principle idea of these methods is to allocate a potential to each point of the configuration space. This potential field consists of a superposition of an attracting potential (the goal) and a repulsive potential (the obstacles). By incorporating the potential field in the heuristic, distances to obstacles can be tuned in a more precise way. Furthermore, the generation of trajectories can be accelerated by lessening the likelihood of futilely exploring paths leading to obstacles that may appear to be less costly when only considering straight line distances. In this paper, the transitions between two succeeding steps are based on Gaussian Processes with empirically derived parameters. Possible future work will therefore consist of an evaluation of various transition models. This includes varying and evaluating diverse parameter configurations or altogether testing various approaches to supervised learning such as neural networks.

REFERENCES

[n. d.]. Gaussian Process Dynamical Models for Human Motion. 30 ([n. d.]).

2015. Improving A* Walk Trajectories with B-splines and Motion Capture for Manual Assembly Verification. *Procedia CIRP* 33 (2015), 364 – 369. 9th CIRP Conference on Intelligent Computation in Manufacturing Engineering - CIRP ICME '14.

Philipp Agethen, Michael Otto, Felix Gaisbauer, and Enrico Rukzio. 2016. Presenting a Novel Motion Capture-based Approach for Walk Path Segmentation and Drift Analysis in Manual Assembly. *Procedia CIRP* 52 (2016), 286–291.

Shailen Agrawal and Michiel van de Panne. 2016. Task-based locomotion. *ACM Transactions on Graphics* 35, 4 (2016), 1–11.

Richard Bowden. 2000. Learning statistical models of human motion. In *IEEE Workshop on Human Modeling, Analysis and Synthesis, CVPR*, Vol. 2000.

Armin Bruderlin and Lance Williams. 1995. Motion signal processing. In *Computer graphics proceedings (Annual conference series)*, Susan G. Mair and Robert Cook (Eds.). Association for Computing Machinery, New York, NY, 97–104.

Maike Buchin, Anne Driemel, Marc Van Kreveld, and Vera Sacristán. 2011. Segmenting trajectories: A framework and algorithms using spatiotemporal criteria. *Journal of Spatial Information Science* 2011, 3 (2011), 33–63.

Joel Chestnutt, James Kuffner, Koichi Nishiwaki, and Satoshi Kagami. 2003. Planning Biped Navigation Strategies in Complex Environments. *Proceedings of the 2003 International Conference on Humanoid Robots* (2003).

J. Chestnutt, M. Lau, G. Cheung, J. Kuffner, J. Hodgins, and T. Kanade. 2006. Footstep Planning for the Honda ASIMO Humanoid. In *IEEE International Conference on Robotics and Automation*. IEEE, [Pitscataway, N.J.], 629–634.

Min Gyu Choi, Jehee Lee, and Sung Yong Shin. 2003. Planning biped locomotion using motion capture data and probabilistic roadmaps. *ACM Transactions on Graphics* 22, 2 (2003), 182–203.

Simon Clavet. 2016. Motion matching and the road to next-gen animation. https://www.gdcvault.com/play/1023280/Motion-Matching-and-The-Road

CloudCompare. 2018. CloudCompare (version 2.9.1) [GPL software]. https://www.danielgm.net/cc/

Arjan Egges and Ben van Basten. 2010. One step at a time: animating virtual characters based on foot placement. *The Visual Computer* 26, 6-8 (2010), 497–503.

Alessandro Gasparetto, Paolo Boscariol, Albano Lanzutti, and Renato Vidoni. 2015. Path planning and trajectory planning algorithms: A general overview. In *Motion and operation planning of robotic systems*. Springer, 3–27.

Roy Glasius, Andrzej Komoda, and Stan CAM Gielen. 1995. Neural network dynamics for path planning and obstacle avoidance. *Neural Networks* 8, 1 (1995), 125–133.

Peter Hart, Nils Nilsson, and Bertram Raphael. 1968. A formal basis for the heuristic determination of minimum cost paths. *IEEE transactions on Systems Science and Cybernetics* 4, 2 (1968), 100–107.

Dirk Helbing, Illés Farkas, and Tamás Vicsek. 2000. Simulating dynamical features of escape panic. (2000).

Daniel Holden, Taku Komura, and Jun Saito. 2017. Phase-functioned Neural Networks for Character Control. *ACM Trans. Graph.* 36, 4, Article 42 (July 2017), 13 pages.

Eugene Hsu, Kari Pulli, and Jovan Popović. 2005. Style translation for human motion. *ACM Transactions on Graphics (TOG)* 24, 3 (2005), 1082–1089.

Yanrong Hu, Simon X. Yang, Li-Zhong Xu, and M.Q.-H. Meng. 2004. A knowledge based genetic algorithm for path planning in unstructured mobile robot environments. In *IEEE International Conference on Robotics and Biomimetics*. IEEE, 767–772.

Eric Jones, Travis Oliphant, Pearu Peterson, et al. 2001. SciPy: Open source scientific tools for Python. http://www.scipy.org/

L. E. Kavraki, P. Svestka, J. C. Latombe, and M. H. Overmars. 1996. Probabilistic roadmaps for path planning in high-dimensional configuration spaces. *IEEE Transactions on Robotics and Automation* 12, 4 (1996), 566–580.

Lucas Kovar, Michael Gleicher, and Frédéric Pighin. 2002a. Motion graphs. *ACM Transactions on Graphics* 21, 3 (2002).

Lucas Kovar, Michael Gleicher, and Frédéric Pighin. 2002b. Motion graphs. In *ACM transactions on graphics (TOG)*, Vol. 21. ACM, 473–482.

J. J. Kuffner, K. Nishiwaki, S. Kagami, M. Inaba, and H. Inoue. 2002. Footstep planning among obstacles for biped robots. In *2001 IEEE/RSJ International Conference on Intelligent Robots and Systems (IROS 2001)*. IEEE, Piscataway, N.J., 500–505.

Steven M. LaValle. 1998. Rapidly-exploring random trees: A new tool for path planning. (1998).

Christian Mandery, Oemer Terlemez, Martin Do, Nikolaus Vahrenkamp, and Tamim Asfour. 2015. The KIT Whole-Body Human Motion Database. In *International Conference on Advanced Robotics (ICAR)*. 329–336.

Martin Manns, Klaus Fischer, Han Du, Philip Slusallek, and Kosmas Alexopoulos. 2018. A new approach to plan manual assembly. *International Journal of Computer Integrated Manufacturing* 0, 0 (2018), 1–14.

Martin Manns, Stefan Mengel, and Markus Mauer. 2016a. Experimental effort of data driven human motion simulation in automotive assembly. *Procedia CIRP* 44 (2016), 114–119.

Martin Manns, Michael Otto, and Markus Mauer. 2016b. Measuring motion capture data quality for data driven human motion synthesis. *Procedia CIRP* 41 (2016), 945–950.

Néstor Andrés Arteaga Martín, Thomas Bär, and Rainer Stark. 2013. A Reference Framework for Manual Assembly Simulation. In *Smart Product Engineering*, Michael Abramovici and Rainer Stark (Eds.). Springer Berlin Heidelberg, Berlin, Heidelberg, 293–302.

Jianyuan Min and Jinxiang Chai. 2012. Motion graphs++: a compact generative model for semantic motion analysis and synthesis. *ACM Transactions on Graphics* 31, 6 (Nov. 2012), 1.

Soraia Musse, Vinicius Cassol, and Claudio Jung. 2012. Towards a quantitative approach for comparing crowds. *Computer Animation and Virtual Worlds* 23, 1 (2012), 49–57.

Jan Ondřej, Julien Pettré, Anne-Hélène Olivier, and Stéphane Donikian. 2010. A Synthetic-vision Based Steering Approach for Crowd Simulation. *ACM Trans. Graph.* 29, 4, Article 123 (July 2010), 9 pages.

F. Pedregosa, G. Varoquaux, A. Gramfort, V. Michel, B. Thirion, O. Grisel, M. Blondel, P. Prettenhofer, R. Weiss, V. Dubourg, J. Vanderplas, A. Passos, D. Cournapeau, M. Brucher, M. Perrot, and E. Duchesnay. 2011. Scikit-learn: Machine Learning in Python. *Journal of Machine Learning Research* 12 (2011), 2825–2830.

Nicolas Perrin. 2018. *Biped Footstep Planning*. Springer Netherlands, Dordrecht, 1–21.

Janko Petereit, Thomas Emter, Christian W Frey, Thomas Kopfstedt, and Andreas Beutel. 2012. Application of Hybrid A* to an autonomous mobile robot for path planning in unstructured outdoor environments. In *Proceedings of ROBOTIK 2012; 7th German Conference on Robotics*.

Craig W. Reynolds. 1999. Steering behaviors for autonomous characters. In *Game developers conference*, Vol. 1999. 763–782.

Luis Molina Tanco and Adrian Hilton. 2000. Realistic synthesis of novel human movements from a database of motion capture examples. In *Workshop on Human Motion. Proceedings.* IEEE, 137–142.

Ben J. H. van Basten, Sybren A. Stüvel, and Arjan Egges. 2011. A Hybrid Interpolation Scheme for Footprint-driven Walking Synthesis. In *Proceedings of Graphics Interface 2011 (GI '11)*. 9–16.

Michiel van de Panne. 1997. From Footprints to Animation. *Computer Graphics Forum* 16, 4 (1997), 211–223.

Jur Van Den Berg, Jamie Snape, Stephen J Guy, and Dinesh Manocha. 2011. Reciprocal collision avoidance with acceleration-velocity obstacles. In *Robotics and Automation (ICRA), 2011 IEEE International Conference on*. IEEE, 3475–3482.

He Wang, Jan Ondřej, and Carol O'Sullivan. 2016. Path Patterns: Analyzing and Comparing Real and Simulated Crowds. In *Proceedings of the 20th ACM SIGGRAPH Symposium on Interactive 3D Graphics and Games (I3D '16)*. 49–57.

H. Wang, J. Ondřej, and C. O'Sullivan. 2017. Trending Paths: A New Semantic-Level Metric for Comparing Simulated and Real Crowd Data. *IEEE Transactions on Visualization and Computer Graphics* 23, 5 (2017), 1454–1464.

S. Yi, H. Li, and X. Wang. 2015. Pedestrian Travel Time Estimation in Crowded Scenes. In *2015 IEEE International Conference on Computer Vision (ICCV)*. 3137–3145.